World Academy of Science, Engineering and Technology
International Journal of Aerospace and Mechanical Engineering
Vol:9, No:7, 2015

Mixing Behaviors of Shear-Thinning Fluids in Serpentine-Channel Micromixers

Rei-Tang Tsai, Chih-Yang Wu, Chia-Yuan Chang, Ming-Ying Kuo

Abstract**—**This study aims to investigate the mixing behaviors of deionized (DI) water and carboxymethyl cellulose (CMC) solutions in C-shaped serpentine micromixers over a wide range of flow conditions. The flow of CMC solutions exhibits shear-thinning behaviors. Numerical simulations are performed to investigate the effects of the mean flow speed, fluid properties and geometry parameters on flow and mixing in the micromixers with the serpentine channel of the same overall channel length. From the results, we can find the following trends. When convection dominates fluid mixing, the curvature-induced vortices enhance fluid mixing effectively. The mixing efficiency of a micromixer consisting of semicircular C-shaped repeating units with a smaller centerline radius is better than that of a micromixer consisting of major segment repeating units with a larger centerline radius. The viscosity of DI water is less than the overall average apparent viscosity of CMC solutions, and so the effect of curvature-induced vortices on fluid mixing in DI water is larger than that in CMC solutions for the cases with the same mean flow speed.

Keywords**—**Microfluidics, mixing, non-Newtonian fluids, curved channel, vortex.

I. Introduction

MOST of microfluidic systems in applications may treat biofluids with non-Newtonian fluid behaviors [1], [2]. However, there are relatively less papers investigating the mixing behaviors of non-Newtonian fluids in micromixers for applications in the micro total analysis systems (μ-TAS). Pathak et al. [1] study the flow instability and mixing of the elastic fluid flowing through a zigzag microchannel. Lam et al. [2] investigate the micromixer based on viscoelastic flow instability. Srisamran and Devahastin [3] show that the impinging streams of shear-thinning fluid with lower flow behavior index may cause smaller recirculating zone and less mixing enhancement. Aubin et al. [4] investigate the effect of geometrical characteristics of microchannels on residence time distributions and axial dispersion for Newtonian and shear-thinning fluids.

In this work, we aim to study the flow and mixing behaviors of non-Newtonian fluids in a C-shaped serpentine micromixer (CSM) constructed by C-shaped repeating units shown in Fig. 1. It is well known that the main feature of the fluid flow in a curved channel is the recirculating (or "vortex") flow due to centrifugal forces on the cross section of the curved channel and the lateral flow provides high heat and mass-transfer rates so as to enhance heat transfer or mixing in laminar flow regimes [5]-[8]. The lateral flow appears a pair of counter-rotating symmetrical vortices called corner vortices and new pairs of counter-rotating vortices appear as the Dean number beyond a critical value [9]. The Dean number is defined as:

$$De = Re\sqrt{d_h / R_c}\ , \tag{1}$$

where Re is the Reynolds number representing the ratio of inertia force to viscous force, d_h and R_c are the hydraulic diameter and the center-line radius of the curved channel, respectively. For comparison purpose, the Newtonian fluid counterparts are also considered. In this work, the deionized (DI) water is used as the Newtonian fluid, while the non-Newtonian fluid considered is the carboxymethylcellulose (CMC) solution that exhibits shear-thinning behavior. We use the power-law model to describe the relationship between the shear stress tensor ($\boldsymbol{\tau}$) and the shear rate tensor ($\dot{\boldsymbol{\gamma}}$) of CMC solutions [3]:

$$\boldsymbol{\tau} = -\left[\ m\ \left|\sqrt{\tfrac{1}{2}(\dot{\gamma}:\dot{\gamma})}\right|^{\,n-1}\right]\ \dot{\boldsymbol{\gamma}} \tag{2}$$

where m denotes the consistency coefficient and n denotes the flow behavior index. The m and the n of 100 ppm CMC solution [3] are similar to those of human blood [10]. Furthermore, the m equals to the viscosity (μ_{DI}) and the n equals to 1 for DI water. The apparent viscosity (μ_a) of CMC solution is calculated as:

$$\mu_a = m\ \left|\dot{\boldsymbol{\gamma}}\right|^{\,n-1} \tag{3}$$

In this work, we investigate the mixing behaviors caused by the vortex flows due to centrifugal force in serpentine-channel micromixers over a wide range of flow conditions; the effects of the radius (R_c), the angular range and the number of the C-shaped repeating units are taken into account.

II. Micromixer Design

The micromixer considered consists of the inlets with a length L_i of 400 μm, the straight microchannel from the inlets to the first curved segment with a length of L_e = 240 μm, the first and the last curved segments with a center-line radius R_c over the angular range from 0° to θ_c, and other N_c curved segments (i.e. C-shaped repeating units) with a center-line radius R_c over the angular range from 0° to θ_m. When θ_m >180°, the C-shaped repeating unit is a major segment curved channel. We call the CSM with θ_c = 45° and θ_m = 270° a major segment serpentine

Rei-Tang Tsai, Chia-Yuan Chang, Ming-Ying Kuo and C.-Y. Wu are with the Department of Mechanical Engineering, National Cheng Kung University, Tainan, Taiwan 701, ROC (phone: 886-62757575-62151; fax: 886-6-2352973; e-mail: n1891125 @ ccmail. ncku. edu. tw, oscar-7895@ hotmail. com, kuomying @ gmail.com, cywu@mail.ncku.edu.tw).

micromixer (MSSM), as shown in Fig. 1 (a), and call the CSM with $\theta_c = 0°$ and $\theta_m = 180°$ a semicircular serpentine micromixer (SCSM), as shown in Fig. 1 (b). The microchannel has a square cross section of W_m = 120 μm by H = 120 μm, except that each of the inlets has a rectangular cross section of W_i = 40 μm by H = 120 μm. The serpentine channel consisting of the C-shaped repeating units is the main part in which mixing is enhanced.

To investigate the effects of the R_c and the θ_m, we compare the performance of the MSSM-180/11 shown in Fig. 1 (a) and that of the SCSM-90/34 shown in Fig. 1 (b), where the first number and the second number after MSSM or SCSM denote the R_c (μm) and the N_c, respectively. The N_c is determined by the R_c and the θ_m based on the same overall channel length of 11000 μm. A single microlithography process may fabricate the CSM's and the mixing behaviors can be observed by using spectral confocal microscope imaging system.

III. Numerical Simulations

In this work, the numerical simulation of the flow and mixing in the micromixer is performed by using the commercial codes, CFD-ACE+ (CFD Research Corporation, CA, USA). The governing equations include the continuity equation, the momentum equation with the shear stress tensor given by (2) and the species diffusion equation for isothermal steady incompressible flow expressed as:

$$\nabla \cdot \boldsymbol{V} = 0\,, \tag{4}$$

$$\rho\left(\boldsymbol{V}\cdot\nabla\right)\boldsymbol{V} = -\nabla p - \left(\nabla\cdot\boldsymbol{\tau}\right), \tag{5}$$

$$\left(\boldsymbol{V}\cdot\nabla\right) c = D\nabla^2 c\,, \tag{6}$$

respectively, where $\boldsymbol{V} = (u, v, w)$ is the velocity vector, ρ the fluid density, p the pressure, c the mole fraction of Rhodamine 6G solution, and D the diffusion coefficient of Rhodamine 6G in DI water or in CMC solutions. The no-slip condition is imposed on all solid walls, and the pressure at the exit is set to be 1 atm. The SIMPLEC algorithm is used for pressure-velocity coupling, and the spatial difference is carried out with the second order upwind scheme with limiter. Furthermore, the stopping criterion of iterative computation is that relative residual of each variable is less than 0.0001.

In this work, the Newtonian fluid considered is the DI water with density, ρ = 997 kgm^{-3}, and viscosity, μ_{DI} = 0.00097 Pa s. The shear-thinning fluids considered are the 100 ppm CMC solution in water with m = 0.00383 Pa s^n and n = 0.9512, and the 500 ppm CMC solution in water with m = 0.00849 Pa s^n and n = 0.8229 [3]. The density of CMC solutions used in the simulation is 1000 kgm^{-3}. Besides, we consider equal flow rate at both inlets, and so the mixing ratio is 1:1. The mole fraction of fluid at inlet A is set to be 1 and that at inlet B is set to be 0. The diffusion coefficients of Rhodamine 6G in DI water and in CMC solutions are 2.8×10^{-10} m^{-2}s^{-1}[11] and 2.0×10^{-10} m^{-2}s^{-1} [12], respectively.

To quantify and compare the mixing performance, the degree of mixing [13], M, at each cross section of the micromixer are calculated as:

$$M = 1 - \frac{\sigma}{\sigma_0}\,, \tag{7}$$

where σ denotes the standard deviation of mole fraction at a transverse cross section defined as:

$$\sigma^2 = \frac{1}{N}\sum_{i=1}^{N}(c_i - \bar{c})^2 \tag{8}$$

with N denoting the total number of sampling, c_i the mole fraction at a position on the cross section considered and $\bar{c}$ the average of c_i. When the two fluids are segregated, the standard deviation can be expressed by:

$$\sigma_0^2 = \bar{c}\,(1-\bar{c}) \tag{9}$$

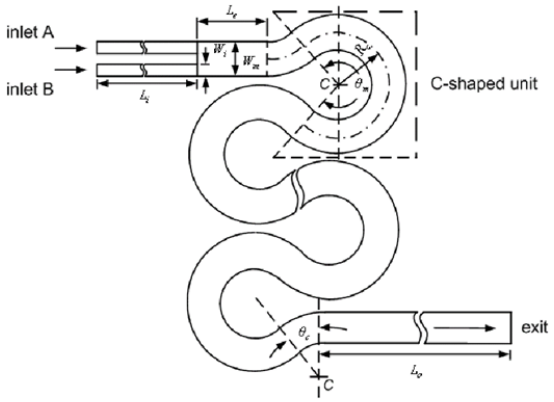

(a)

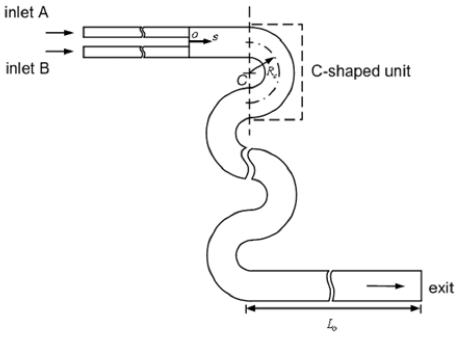

(b)

Fig. 1 (a) Schematic diagram of the MSSM-180/11 with θ_c = 45° and θ_m = 270°. (b) Schematic diagram of the SCSM-90/34 with θ_c = 0° and θ_m = 180°

In this work, we estimate the mixing efficiency of a micromixer by calculating the degree of mixing at the exit cross section (M_{exit}).

To characterize the viscous effect of the non-Newtonian fluid in the microchannel, we adopt the generalized Reynolds number defined as:

$$Re_g = \frac{\rho \bar{u}^{2-n} d_h{}^n}{m\{(24n+\xi)/(24+\xi)n\}^n \xi^{n-1}} \quad (10)$$

where $\bar{u}$ is the mean flow speed, the geometrical parameter ξ = 7.113 for the channel with a square cross section [14]. For a Newtonian fluid, $m = \mu$, $n = 1$, and so $Re_g = Re = \rho \bar{u} d_h / \mu$.

IV. Results and Discussion

To find the optimal size of cells for simulations, four different structured grid systems were tested for the SCSM-90/34. Fig. 2 shows the profiles of velocity component u on a cross section of the channel and Fig. 3 shows the average of the concentration distribution on a cross section of the channel for various values of Re_g. Those values of Re_g are selected to cover the regimes of flow from the diffusion domination to the convection domination of mixing in the CSM's. The values of $\bar{u}$ and De corresponding to those Re_g are listed in Table I, where the Dean number for non-Newtonian fluids is defined as:

$$De = Re_g \sqrt{d_h / R_c} \quad (11)$$

From Figs. 2 and 3, it is seen that the simulation results obtained by the grid systems using cells with all sides less than or equal to 5 μm are in good agreement. To reduce the computation cost, we use structured cells with the longest side equal to 5 μm in the following simulations.

Before comparing the mixing behaviors of DI water and CMC solutions in the CSM's, we compare the mixing performance of the MSSM-180/11, the SCSM-90/34 and a straight channel micromixer (SCM). The channel width, height and the overall channel length of the main channel of the three mixers are the same. Fig. 4 shows the degrees of mixing in DI water at the exit cross section and the pressures applied between the inlets and the exit of the three micromixers under the flow conditions of $\bar{u}$ = 0.0008, 0.0024, 0.0081, 0.0243, 0.0729, 0.2187, and 0.6561 m/s. When the $\bar{u}$ is very small ($\bar{u} \le 0.0081$ m/s), the mixing is caused mainly by diffusion which does not rely on the channel geometric, and so the degree of mixing of the three micromixers is almost equal. Because of the same cross section size of the three micromixers, the pressures applied of those micromixers are very similar to each other until the lateral convection become significant, as shown in Fig. 4 (b). The long residence time is beneficial to diffusion and leads to a good mixing efficiency as the $\bar{u}$ is small. Since the residence time decreases with the increase of $\bar{u}$, the degree of mixing of the CSM's decreases with the increases of $\bar{u}$ until the effect of corner vortices becomes dominant at a middle value of $\bar{u}$, as shown in Fig. 4 (a). When the $\bar{u}$ is larger than the value, the fluid mixing in the CSM's are enhanced by corner vortices, especially for the CSM with a smaller centerline radius and a higher number of C-shaped units, as shown in Figs. 4 (a) and 5. The critical value of Re for the regime transition of diffusion dominate to convection dominate is about 3 for DI water, as shown in Fig. 4 (a). The degree of mixing of the SCM, by contrast, decreases with the increase of $\bar{u}$ monotonously. This is because the flow in the SCM does not have the curvature-induced vortices on the transverse cross sections. Besides, from the definition of the Dean number, we readily see that the De is proportional to the Re for the cases with the parameters d_h and R_c fixed. Fig. 4 (a) shows that the M_{exit} of the SCSM-90/34 is greater than that of the MSSM-180/11 as the lateral convection becomes dominant. This is because the centrifugal force increases with the decrease of R_c and so the decrease of R_c enhances lateral convection and fluid mixing. Therefore, we adopt the SCSM-90/34 for the following investigations.

When the $\bar{u}$ is large enough, the lateral convection due to centrifugal force can efficiently distort and increase the interface between fluids in a few C-shaped units, as shown Fig. 5. The counter-rotating symmetrical vortices in the C-shaped units with a smaller R_c is much stronger than those in the C-shaped units with a larger R_c, as shown in Fig. 5 (c). The comparison shown in Figs. 4 (a) and 5 (b) reveals that the effect of a small channel radius on fluid mixing is larger than that of a large θ_m of the C-shaped unit on fluid mixing.

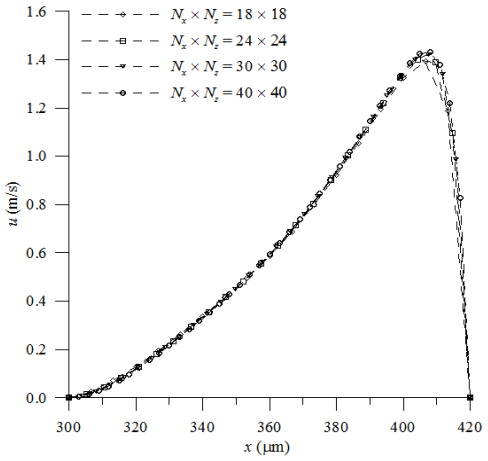

Fig. 2 Profiles of velocity component v on a vertical cross section (300 μm $\le x \le$ 420 μm, y = 240 μm, z = 60 μm) of SCSM-90/34 for the shear-thinning flow (CMC 500 ppm Re_g = 57.76)

TABLE I
Values of $\bar{u}$ and Corresponding Values of Reynolds Number and Dean Number for the Cases Considered

	DI Water		CMC 100ppm Solution		CMC 500ppm Solution	
$\bar{u}$(m/s)	Re	De	Re_g	De	Re_g	De
0.0008	0.0987	0.1139	0.0298	0.0345	0.0215	0.0248
0.0024	0.2960	0.3418	0.0944	0.1090	0.0782	0.0903
0.0243	3.0000	3.4637	1.0715	1.2372	1.1945	1.3793
0.0729	9.0000	10.392	3.3919	3.9166	4.3540	5.0275
0.2187	26.975	31.147	10.725	12.385	15.849	18.301
0.6561	80.924	93.442	33.948	39.200	57.761	66.697

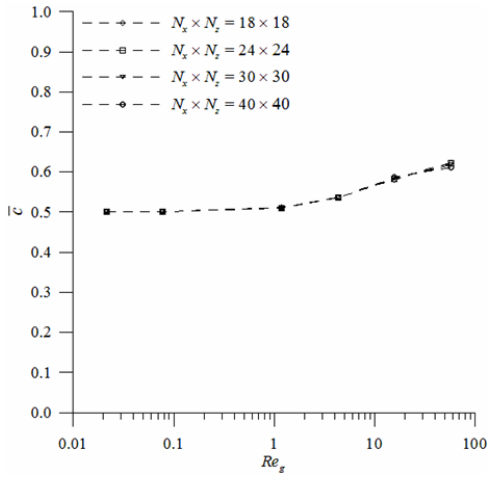

Fig. 3 Averages of concentrations for the shear-thinning flow (CMC 500 ppm) on a vertical cross section at the exit of the first C-shaped unit of the SCSM-90/34for various values of Re_g

The main feature of the flow in a curved segment is the counter-rotating symmetrical vortices on the transverse cross section of the curved channel. Fig. 6 shows the lateral convection of DI water and CMC solutions on the vertical plane at $\theta = 90°$ of three C-shaped units in the SCSM-90/34 for the cases with $\overline{u}$ = 0.2187 m/s. For the cases considered, there is only one pair of counter-rotating vortices on each of the cross sections shown. The value of *De* for this case shown in Table I is much less than the critical Dean number for the appearance of new vortex pair [10]. The flow patterns on the vertical plane at $\theta = 90°$ of the fifth and the seventh C-shaped units are almost identical, and so the flow in the C-shaped serpentine channel of the SCSM-90/34 is nearly periodical. Comparison of the flow patterns on the vertical plane at $\theta = 90°$ of the fifth and the sixth C-shaped units shows that the direction of counter-rotating vortices can be switched by changing the sign of curvature. Furthermore, from Fig. 6 we can see that the largest lateral convection on the cross sections appears in DI water and the lateral convection of 500 ppm CMC solution is larger than that of 100 ppm CMC solution at this mean flow speed. That is, the magnitude of the lateral convection increases with the decrease of the apparent viscosity. The inertial forces of the three fluids flowing along the SCSM-90/34 are almost the same due to the equal value of $\overline{u}$. Thus, the difference of the lateral convection is caused by viscous forces in the three fluids and shall be explained by the shear rate and apparent viscosity. The viscosity in the vortex zone is higher due to the lower shear rate; this reduces vortex flow. Thus, the curvature-induced vortices on the transverse cross sections shown in Fig. 6 of the shear-thinning flow are weaker than those of Newtonian fluid flow at the same value of $\overline{u}$. A similar flow behavior has also been found by Srisamran and Devahastin [3].

The average apparent viscosity of CMC solutions over a vertical cross section is defined as:

$$\mu_{a,avg} = \frac{1}{N}\sum_{i=1}^{N} \mu_{a,i}\,, \tag{12}$$

where N denotes the total number of sampling and $\mu_{a,i}$ denotes the apparent viscosity at a position on the cross section considered. The $\mu_{a,i}$ of shear thinning fluids depends on the shear rate that can be calculated by the codes CFD-ACE+. Fig. 7 (a) shows that the ratio $\mu_{a,avg}/\mu_{DI}$ vary periodically, and the variation is very small. Thus, the curvature of the channel has only moderate influence on $\mu_{a,avg}$. Next, we further take the average of $\mu_{a,avg}$ over a C-shaped unit and defined the resulting value as the overall average of apparent viscosity, $\overline{\mu}_{a,avg}$. The ratios of the $\overline{\mu}_{a,avg}$ of CMC solution to the viscosity of DI water are shown in Fig. 7 (b) for a wide range of flow conditions. Fig. 7 (b) shows the slope of the viscosity curve of 500 ppm CMC solution is larger than that of 100 ppm CMC solution, the two curves of the $\overline{\mu}_{a,avg}$ / μ_{DI} intersect at a certain mean flow speed between 0.0081 and 0.0243 m/s, and the 100 ppm CMC solution has a larger viscosity for a case with a higher flow speed.

Fig. 8 shows the degrees of mixing (*M*) for DI water and CMC solutions at the end of each C-shaped unit of the SCSM-90/34. When diffusion dominates fluid mixing for the cases with $\overline{u}$ = 0.0081 m/s, the curves of *M* with respect to the number of C-shaped units are approximately linear. Besides, the slope of the *M* curve of DI water is larger than that of CMC solutions, because the diffusion coefficient of Rhodamine 6G in DI water is larger than that in CMC solutions. When fluid mixing is dominated by convection for the cases with $\overline{u}$ = 0.2187 m/s, the viscosity plays an important role and the curvature-induced vortices enhance fluid mixing effectively. Thus, the curves of *M* with respect to the number of C-shaped units for the cases with $\overline{u}$ = 0.2187 m/s are beyond those for the cases with $\overline{u}$ = 0.0081 m/s, as shown in Fig. 8. Since the viscosity of 500 ppm CMC solution is less than that of 100 ppm CMC solution and larger than that of DI water, the *M* curve of 500 ppm CMC solution is below that of DI water and beyond that of 100 ppm CMC solution.

Fig. 9 shows the degrees of mixing in DI water and CMC solutions at the exit and the pressures applied between the inlets and the exit of the SCSM-90/34 and the SCM for the cases with $\overline{u}$ = 0.0008, 0.0024, 0.0081, 0.0243, 0.0729, 0.2187, and 0.6561 m/s. From Fig. 9 (a) we can find the following trends. (i) When diffusion dominates the fluid mixing, the degrees of mixing of the SCM and SCSM-90/34 are almost equal. Besides, the degrees of mixing of CMC solutions are smaller than that of DI water, because the diffusion coefficient of Rhodamine 6G in DI water is larger than that in CMC solutions. (ii) For the cases with the SCSM-90/34, we can see that the degree of mixing of DI water is larger than that of CMC solutions inflows considered. This is because DI water has the larger diffusion coefficient for the situation dominated by diffusion and has the larger effect of curvature-induced vortices on the transverse cross section for the situation dominated by convection. Furthermore, according to the result shown in Fig. 7 (b), the overall average apparent viscosity of 500 ppm CMC solution is larger than that of 100 ppm CMC solution while $\overline{u} \le$ 0.0081 m/s. Hence, the effect of the curvature-induced vortices and the

degree of mixing of 500 ppm CMC solution are less than those of 100 ppm CMC solution at those flow conditions. When the $\overline{u}$ increase further ($\overline{u} \geq 0.0243$ m/s), the overall average apparent viscosity of 500 ppm CMC solution is less than that of 100 ppm CMC solution and so the effect of curvature-induced vortices and the degree of mixing of the former are larger than those of the latter.

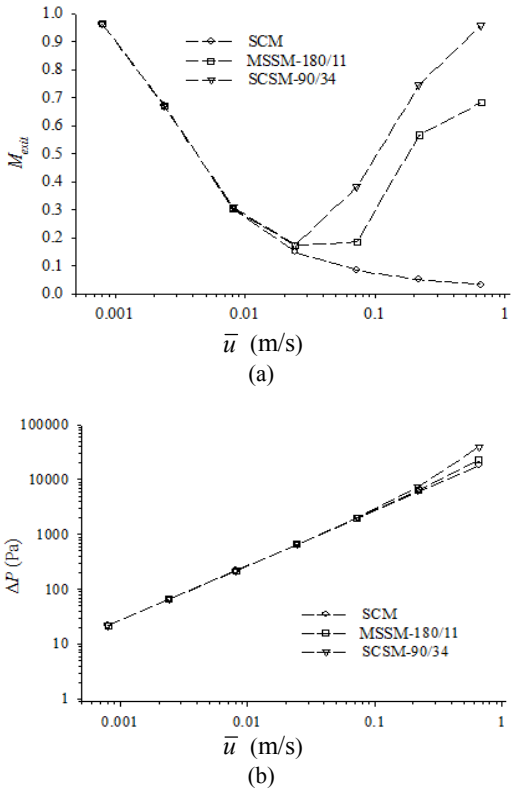

Fig. 4 (a) Degrees of mixing at the exits and (b) pressures applied between the inlets and the exit of the SCM, the MSSM-180/11 and the SCSM-90/34 for the cases with $\overline{u}$ = 0.0008, 0.0024, 0.0081, 0.0243,0.0729, 0.2187, and 0.6561 m/s, n = 1 and $m = \mu_{DI}$ (DI water)

Fig. 9 (b) shows the pressure applied increases with the increases of $\overline{u}$ and/or apparent viscosity. The pressure applied to DI water is less than that applied to CMC solutions in those mean flow speeds considered. Besides, the pressure applied to 500 ppm CMC solution is larger than that applied to 100 ppm CMC solution as $\overline{u} \leq 0.0081$ m/s and the pressure applied to the former is less than that applied to the latter as $\overline{u} \geq 0.0243$ m/s. Because of the same cross section size, the pressure applied to the flow in the SCSM-90/34 and the SCM is nearly the same when the effect of convection is minor. While the effect of convection is significant, the pressure applied to the flow in the SCSM-90/34 is greater than that in the SCM, and their difference increases with the increase of $\overline{u}$. This is because a larger pressure applied to the fluid in the SCSM-90/34 is required to overcome the larger wall shear stress due to the higher velocity gradient in the C-shaped units. However, from Fig. 9 we can see that it is an acceptable tradeoff between the increase of the pressure applied and the enhancement of the fluid mixing in the SCSM-90/34, especially for the case with a large mean flow speed.

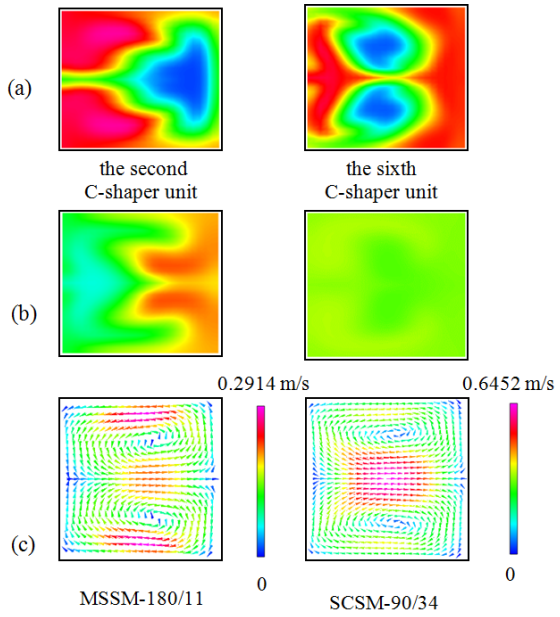

Fig. 5 Concentration distributions of the MSSM-180/11 and the SCSM-90/34 (a) on the cross section corresponding to the channel length of the main channel, L_{curve} = 1696 μm, (b) on the cross section at the exit and (c) flow patterns on the cross section at θ = 90° of the first C-shaped unit for the cases with $\overline{u}$ =0.6561 m/s, n = 1 and $m = \mu_{DI}$ (DI water)

V. Conclusion

In this work, we investigate the effects of the mean flow speed, fluid properties and geometry parameters, the radius and the angular range of the C-shaped repeating units of the serpentine channel, on fluid mixing. The results show that the mixing efficiency of the serpentine micromixers consisting of semicircular C-shaped repeating units with a smaller centerline radius is better than that of other curved channel micromixers of the same overall channel length. When convection dominates fluid mixing, the curvature-induced vortices enhance fluid mixing effectively. The critical value of *Re* for the regime transition of diffusion dominate to convection is about 3 for DI water. Since the apparent viscosities of CMC solutions decrease with the increase of the shear rate, the CMC solutions and DI water flowing in the serpentine at the same speed have different ratios of inertial and viscous forces and display different mixing efficiencies. From the results over a wide range of flow speeds, we can see that the effects of curvature-induced vortices and the degree of mixing of DI water are larger than those of CMC solutions for the cases with the same mean flow speed. Furthermore, while the effect of lateral convection is significant on the fluid mixing, the average apparent viscosity of 500 ppm CMC solution is less than that of 100 ppm CMC solution and so the degree of mixing of 500 ppm CMC solution are larger than those of 100 ppm CMC solution.

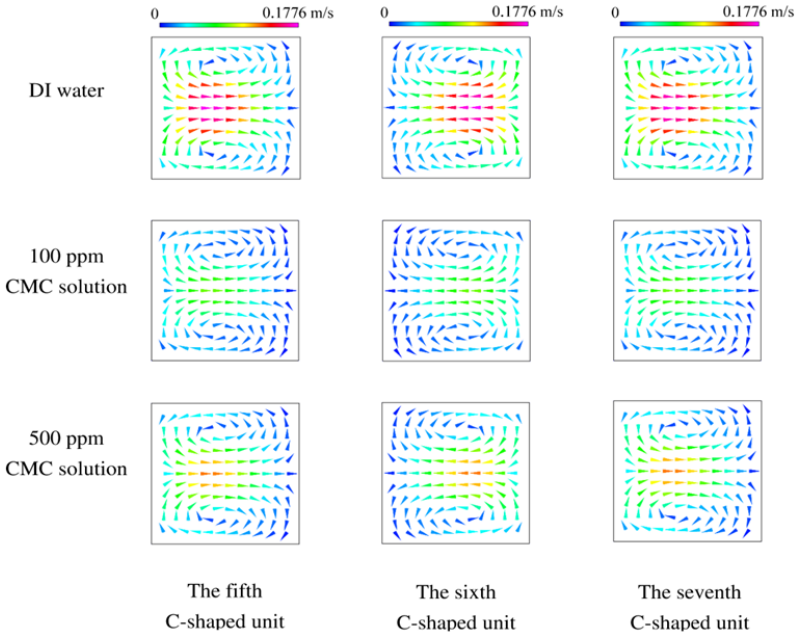

Fig. 6 Flow patterns on the cross sections at $\theta = 90°$ of the fifth, the sixth and the seventh C-shaped units of the SCSM-90/34 for the case with $\bar{u}$ = 0.2187 m/s

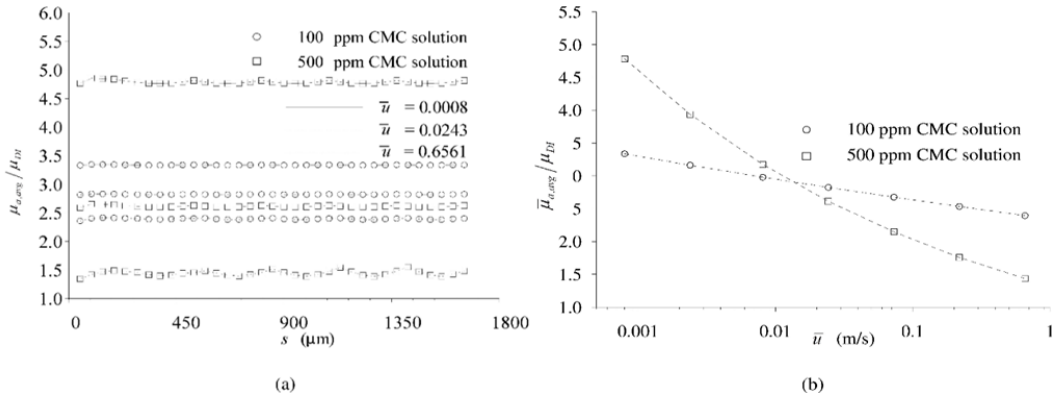

Fig. 7 (a) Ratios of the average apparent viscosity of CMC solutions on the vertical cross section of the SCSM-90/34 to the viscosity of DI water for the cases with $\bar{u}$ = 0.2187 m/s. (b) Ratios of the overall average apparent viscosity of CMC solutions on the vertical cross section of each C-shaped unit of the SCSM-90/34 to the viscosity of DI water for the cases with $\bar{u}$ = 0.0008, 0.0024, 0.0081, 0.0243, 0.0729, 0.2187, and 0.6561 m/s

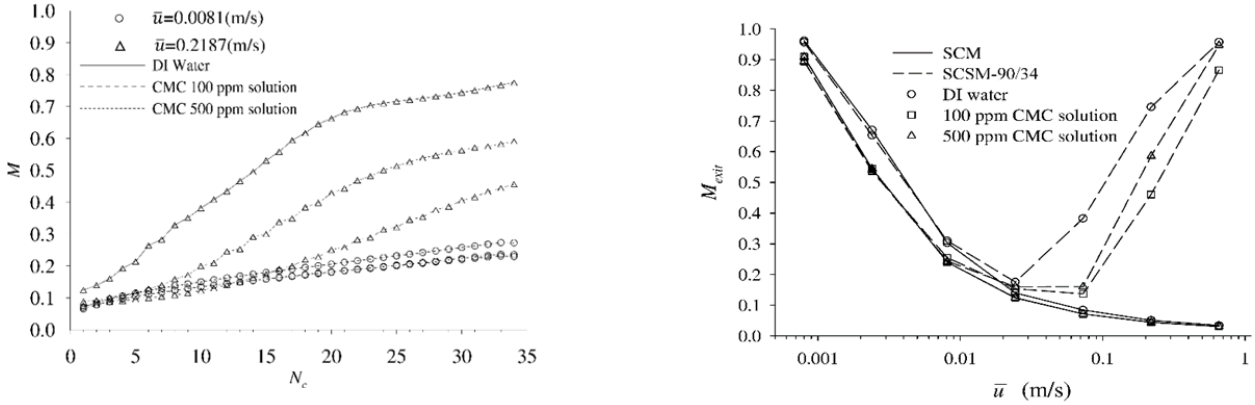

Fig. 8 Degrees of mixing of DI water and CMC solutions at the end of each C-shaped unit of the SCSM-90/34 for the cases with $\bar{u}$ = 0.0081 and 0.2187 m/s

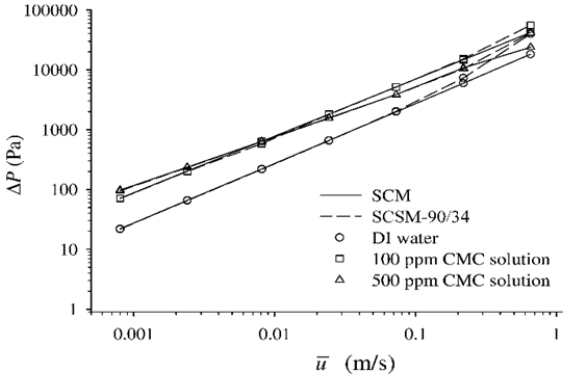

(**b**)

Fig. 9 (a) Degrees of mixing of DI water and CMC solutions at the exit and (b) pressures of DI water and CMC solutions applied between the inlets and the exit of the SCSM-90/34 and the SCM for the cases with $\overline{u}$ = 0.0008, 0.0024, 0.0081, 0.0243, 0.0729, 0.2187, and 0.6561 m/s

ACKNOWLEDGMENT

This work is supported by the Ministry of Science and Technology of the Republic of China on Taiwan through Grant NSC 101- 2221 - E - 006 - 108 - MY3.

REFERENCES

[1] J. A. Pathak, D. Ross, and K. B. Migler, "Elastic flow instability, curved streamlines, and mixing in microfluidic flows," *Phys. Fluids*, vol. 16, pp. 4028-4034, 2004.
[2] Y. C. Lam, H. Y. Gan, N. T. Nguyen, and H. Lie, "Micromixer based on viscoelastic flow instability at low Reynolds number," *Biomicrofluidics*, vol. 3, 014106 (14 pages), 2009.
[3] C. Srisamran and S. Devahastin, "Numerical simulation of flow and mixing behavior of impinging streams of shear-thinning fluids," *Chem. Eng. Sci.*, vol. 61, pp. 4884-4892, 2006.
[4] J. Aubin, L. Prat, C. Xuereb, and C. Gourdon, "Effect of microchannel aspect ratio on residence time distributions and the axial dispersion coefficient," *Chem. Eng. process*, vol. 48, 554–559, 2009.
[5] H. Peerhossaini, C. Castelain, and Y. Le Guer, "Heat-exchanger design based on chaotic advection," *Exp. Therm. Fluid Sci.*, vol. 7, pp. 333-344, 1993.
[6] F. Jiang, K. S. Drese, S. Hardt, M. Küpper, and F. Schönfeld, "Helical flows and chaotic mixing in curved microchannels," *AIChE J.,* vol. 50, pp. 2297-2305, 2004. F. Garofalo, A. Adrover, S. Cerbelli, and M. Giona, "Spectral characterization of static mixers. The S-shaped micromixer as a case study," *AIChE J.*, vol. 56, pp. 318-335, 2010.
[7] F. Garofalo, A. Adrover, S. Cerbelli, and M. Giona, "Spectral characterization of static mixers. The S-shaped micromixer as a case study," *AIChE J.*, vol. 56, pp. 318-335, 2010.
[8] C.-Y. Wu and R.-T. Tsai, "Fluid mixing via multi-directional vortices in converging-diverging meandering microchannels with semi-elliptical side walls," *Chem. Eng. J.,* vol. 217, pp. 320-328, 2013.
[9] R. P. Chhabra and J. F. Richardson, *Non-Newtonian Flow, and Applied Rheology: Engineering Applications*. 2nd ed. Butterworth-Heinemann, Oxford, 2008.
[10] F. Fellouah, C. Castelain, A. Ould-El-Moctar, and H. Peerhossaini, "The Dean instability in power-law and Bingham fluids in a curved rectangular duct," *J. Non-Newtonian Fluid Mech.*, vol. 165, pp. 163–173, 2010.
[11] U. Meseth, T. Wohland, R. Rigler, and H. Vogel, "Resolution of fluorescence correlation measurements," *Biophysical J.*, vol. 76, pp. 1619-1631, 1999.
[12] A. L. Ventresca, Q. Cao, and A. K. Prasad, "The influence of viscosity ratio on mixing effectiveness in a two-fluid laminar motionless mixer," *Can. J. Chem. Eng.*, vol. 80, pp. 614-621, 2002.
[13] J. Boss, "Evaluation of the homogeneity degree of mixture," *Bulk Solids Handl.*, vol. 6, pp. 1207-1215, 1986.
[14] F. Delplac and J. C. Leuliet, "Generalized Reynolds number for the flow of power-law fluids in cylindrical ducts of arbitrary cross-section," *Chem. Eng. J.*, Vol. 56, pp. 33-37, 1995.